J. Phys. D: Appl. Phys. **29** (1996) 1014–1020. Printed in the UK

# A particle-in-cell simulation of the breakdown and period doubling thresholds for a RF discharge Ar plasma

**T H Chung†, H J Yoon†, T S Kim† and J K Lee‡**

† Department of Physics, Dong-A University, Pusan 604-714, South Korea
‡ Department of Physics, Pohang University of Science and Technology, Pohang 790-784, South Korea

Received 26 July 1995, in final form 20 December 1995

**Abstract.** RF glow-discharge plasmas provide mild energetic ion bombardment of exposed surfaces. The characteristics of a 10 MHz RF glow-discharge Ar plasma are studied by particle-in-cell simulation. The model simulates a spherical plasma device using a one-dimensional plasma model. The code is used to determine the breakdown voltage, $V_{rf}$, for a given $pd$, where $p$ is the gas pressure and $d$ is the plasma discharge length. These values are then compared with Paschen's law for the DC case. Also, the breakdown voltage as a function of driver frequency is investigated. Due to the nonlinear capacitance of the plasma, the current and voltage waveforms are found to contain higher harmonic components and sub-harmonic components. Above a certain power level of the driver, sub-harmonics which are indicative of a period-doubling (PD) bifurcation are found to become dominant. The PD thresholds for varying $pd$, the magnitude of the current and the voltage of the Fourier-analysed components as a function of applied RF voltages are calculated. The PD threshold is always higher than the breakdown threshold. Finally, the pressure-dependence of the sheath width is discussed.

## 1. Introduction

RF glow-discharge plasmas provide mild energetic ion bombardment of exposed surfaces. The commonly used reactor creates a discharge by radio frequency energy coupled to one electrode of a parallel plate system at pressures between $10^{-2}$ and 10 Torr. At the higher pressure end of this range, the plasma can be well modelled using fluid equations.

Despite the extensive use of gas plasmas, the intricate nature of the gas discharge is poorly understood. This is mainly due to the complexity of the discharge system. Electron processes include energy-dependent ionization, excitation and elastic scattering; electron energy losses to the electrodes due to the inelastic collisions and the attachment with electrode atoms; electron ohmic heating in the sheaths and bulk plasma; stochastic heating by the oscillating electric fields in the sheath; secondary electron emission; and secondary electron–neutral ionization. Ion processes include ion energy losses to the electrodes due to the inelastic collisions with the electrode atoms, ambipolar ion diffusion, ion acceleration in self-consistent sheaths and production of secondary electrons [1].

The particle-in-cell (PIC) technique is an efficient and conceptually simple method of solving a wide variety of complex problems involving a large number of particles moving under the action of self-generated and externally imposed forces. In this work, we present computational results obtained using spherical many-particle simulation models. The simulation code is PDS1 (plasma device spherical one-dimensional) which utilizes a PIC technique plus the Monte Carlo method for the charged particle–neutral collisions [2]. Using the PDS1 code, we will determine the breakdown voltage for given $pd$, where $p$ is the gas pressure and $d$ is the plasma discharge length, and then compare these values with Paschen's law for DC case.

It is observed in RF discharges that a lower gas pressure results in a higher breakdown voltage. The breakdown voltage has a steep negative slope in the region below the Paschen minimum. The breakdown voltage is empirically formulated as a function of $pd$. On the other hand, the breakdown voltage measured on the pseudo-spark device [3] indicates that the breakdown voltage is a function of $p^2d$, the product of the gas pressure squared and the anode–cathode gap distance. Another interesting problem is the variation of the breakdown voltage with the driver RF frequency. The single-particle theory [4] can estimate the breakdown voltage which can be compared

0022-3727/96/041014+07$19.50 

with experimental results. The validity of the single-particle theory for breakdown phenomena will be tested using a PIC simulation.

It is known that a driven nonlinear $RLC$ circuit can exhibit period doubling (PD) and chaos. The nonlinear element in the circuit is a varactor diode whose capacitance varies as a function of the voltage across it [5]. Capacitively coupled RF discharge systems also displayed characteristics similar to those of the nonlinear $RLC$ circuit [6, 7]. In this case, the nonlinear capacitance due to the plasma sheath is known to be the cause of the period doubling and bifurcations.

The chaotic behaviour of the RF discharge system is determined by the driver frequency, the applied RF voltage and the gas pressure, or by the feedback term of the time delay [6]. Such chaotic behaviour is classified as driven chaos. In this study, we investigate the effects of the driver frequency, RF voltage, gas pressure and external circuit parameters on the characteristics of the driven chaos system using PIC simulation. Also, we give some physical explanation of that phenomenon. The electrical characterization of the RF plasma processing system is quite important in order to understand the power dissipation mechanism and to control the ion bombardment.

## 2. Features of the RF breakdown and period doubling phenomena

When a neutral gas is subject to a RF field, the ionization processes can become markedly different from those under a DC field. Although the type of gas and its pressure play just as important a role in the sequence of ionization processes as in the DC case, the frequency ($f$) with which the field is pulsating determines the overall characteristics of the system. The cut-off frequency gives a distinct limit between two different breakdown mechanisms. With $f < f_{co}$ (the cut-off frequency), the electrons are lost mainly according to their mobility towards the electrodes (the mobility-controlled mechanism). With $f > f_{co}$, the electrons are lost mainly by diffusion (the diffusion-controlled mechanism). The cut-off frequency can be determined by solving [4]

$$\frac{d}{2} = \frac{eE_b}{2\pi m f_{co}[\nu_m^2 + (2\pi f_{co})^2]^{1/2}} \qquad (1)$$

where $m$ is the electron mass, $\nu_m$ is the momentum transfer collision frequency and $E_b$ is the breakdown field strength. In the frequency region above the cut-off frequency, two different scalings of the breakdown voltage on the frequency exist. At a high pressure with $\nu_m > 2\pi f$, the breakdown field strength scales as $E_b \propto \nu_m$, whereas at a low pressure with $2\pi f > \nu_m$, $E_b \propto f/\nu_m$ [4]. These scalings will also be tested.

When an electrical system with nonlinear impedance characteristics operates periodically with frequency $f$, higher harmonics will be generated by the nonlinearity at frequencies $2f, 3f, 4f$ and so on, and sub-harmonics will also be generated at frequencies $f/2, 3f/2, 5f/2$ and so on. Above a certain power level of the driver, sub-harmonics

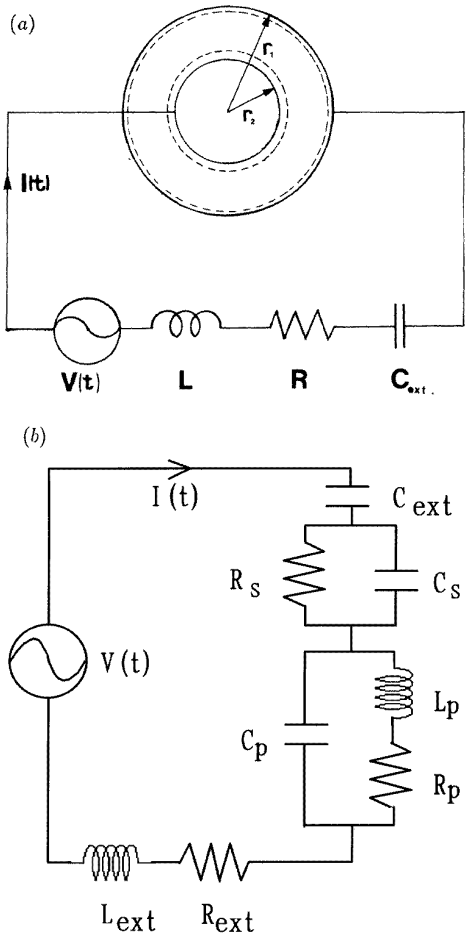


**Figure 1.** (*a*) A Schematic diagram of the simulation device. (*b*) The equivalent circuit representing the RF chamber and the external element.

which are indicative of a period-doubling (PD) bifurcation become dominant [7]. A further increase in the RF voltage level beyond the PD threshold can lead to successive stages of period multiplication that result in the onset of chaos at a finite excitation level. The plot of the PD thresholds for varying $pd$ will be drawn. Period doubling bifurcations manifest themselves in a driven system by an alternation of state variables between different values during successive cycles of the excitation waveforms. This corresponds to the generation of sub-harmonics ($f/2$) and odd multiples of the half-harmonic frequency [7, 8].

Figure 1($a$) is a schematic diagram of the simulation device. One electrode is powered and the other is earthed. It can be seen in figure 1($b$) that the plasma RF chamber is represented by a parallel tuned circuit $L_p, C_p, R_p$, whereas the resistance and the capacitance of both sheaths (inner and outer) are represented by $R_s$ and $C_s$. In addition to these, the external circuit $C_{ext}, L_{ext}, R_{ext}$ contributes to the equivalent circuit parameters. This circuit has two resonance frequencies [9]. The first is the resonance frequency of the parallel circuit $\omega_1 = (L_p C_p)^{-1/2}$ (which is equal to the electron plasma frequency), the second is $\omega_2 = (LC_{eq})^{-1/2}$, where $L$ and $C_{eq}$ are the equivalent

inductance and capacitance of the whole system,

$$C_{eq} = \frac{C_{ext}}{1 + C_{ext}/C_{ch}} \tag{2}$$

where $C_{ch}$ is the equivalent capacitance representing the RF chamber (the bulk plasma and the sheath). Note that $C_{ch}$ is a complex function of the driver frequency ($f$), plasma resistance ($R_p$), the sheath capacitance ($C_s$) and the cell capacitance ($C_p$) [9].

Thus, the charge $Q$ on the capacitor obeys

$$L\frac{\mathrm{d}^2Q}{\mathrm{d}t^2} + R\frac{\mathrm{d}Q}{\mathrm{d}t} + \frac{Q}{C_{eq}} = V(t) \tag{3}$$

where $V(t) = V_{rf}\cos(2\pi f t)$ is the applied voltage and $R$ is the equivalent resistance of the whole system.

Since the sheath capacitance depends on the control parameters in a complicated way, its dependence on the applied RF voltage is not simple [10]. There were some assumptions on the functional dependence of $C_{eq}$ on $V(t)$ [5, 8],

$$C_{eq} = \frac{C_1}{1 + kV_c} \tag{4}$$

where $C_1$ is a constant capacitance and $V_c$ is the voltage across the capacitor $C_{eq}$. Comparing equation (4) with equation (2), we can note that the dependence of $C_{ch}$ on the driver frequency is neglected in this assumption. Equation (3) combined with equation (4) predicts the period-doubling phenomenon analytically, so equation (4) is a possible representation of the nonlinear capacitance. This nonlinear capacitance gives rise to the period doubling. If $V_{rf}$ is greater than some threshold value, the solution of equation (3) has sub-harmonics (multiples of $f/2$); in other words, the period-doubling phenomenon can happen in the discharge current. The value of the period-doubling threshold is a complex function of $L, R, C_p, C_{ext}, C_s$ and $f$. The parameter, $pd$, which specifies the breakdown condition may be related to the system impedance $L, R, C_p$ and $C_s$. The plot of the period-doubling threshold as a function of $pd$ is drawn just as in the case of the breakdown threshold. The analytical theory [8] indicates that the lowest PD threshold occurs at $f = (1/\pi)(LC_{eq})^{1/2}$, that is, two times the resonant frequency of the system. In other words, the driver frequency which doubles the resonance frequency of the system can result in PD easily.

The formation of the plasma sheath is considered to be associated with the difference in motions between highly mobile electrons and heavy positive ions. The sheath capacitance is inversely proportional to the sheath thickness [10]. The nonlinear sheath capacitance may be explained alternatively by taking into account the possibility of the sheath instability which arises when the ion transit time through the sheath is comparable to the RF period [11].

In this study, the period-doubling characteristics are investigated with varying driver amplitude ($V_{rf}$) and driver frequency (in a large range around the resonance frequency of the equivalent circuit). The results obtained are presented in a kind of phase diagram in two-dimensional parameter space ($f, V_{rf}$). Finally, the pressure-dependence of the sheath thickness will be determined [12].

**Table 1.** Simulation parameters.

| |
|---|
| Circuit parameters $L$ = 7.6 $\mu$H, $C_{ext}$ = 10 nF, $f$ = 10 MHz |
| Outer and inner radii of electrode (cm) $r_1$ = 36, $r_2$ = 16 |
| Initial electron density $2 \times 10^6$ cm$^{-3}$ |
| Neutral gas temperature 0.026 eV |
| Secondary electron coefficient ($\gamma$) 0.2 |

Before performing the calculation of the threshold voltage of breakdown and period doubling, the simulation parameters and the operating mode of the system have to be specified. Since the validity of simulation results critically depends on the collision cross section, a more realistic cross section profile is considered [2]. For the energy-dependence of the electron impact cross sections in the PIC–Monte Carlo collision simulation, we employ the approximate values of cross section given in the original PDP1 code [13, 14]. The time step is $\Delta t = 10^{-9}$ s and the mesh size is 0.1 cm. One thousand computer particles (each represents $8 \times 10^6$ real particles) are used as the initial number in the simulation.

We define the breakdown potential as the threshold voltage which makes the number of the computer particles ten times its initial value (in the long run the number saturates). The plasma sheath width is defined as the distance from the electrode to the point where quasi-neutrality of the bulk region ends, that is, where the electric field deviates from zero.

At a low RF discharge voltage, the ionization is provided by plasma electrons and the discharge is in the $\alpha$ mode, whereas at a high RF voltage the ionization is maintained by fast electrons initiated at the RF electrodes and the discharge is in the $\gamma$ mode [15]. This simulation assumes that the RF discharge starts from the pre-ionized state (with electron density of $2 \times 10^6$ cm$^{-3}$ ). Some simulation parameters are listed in table 1.

## 3. Results and discussion

Figure 2 shows the discharge current waveform and its Fourier spectrum. The higher harmonics and sub-harmonics are shown and period doubling is also observed. Figure 3 shows the breakdown voltage as a function of driver frequency for three values of gas pressure, $p = 0.03$, 0.3 and 3 Torr. The cut-off frequency is estimated to be around 3–4 MHz and, for the 10–50 MHz region the breakdown potential increases with the pressure; on the other hand, for the 100–1000 MHz region, it decreases with the pressure. This exhibits the same tendency as that found with the estimation of the single-particle theory. Also, it is observed that the microwave discharge (at 1 GHz) has a lower threshold voltage. This can be accounted for in that the electron density obtained for a given high-frequency power deposited into the plasma is usually higher at microwave than at radio frequencies [16].

Figure 4 shows the breakdown voltage and PD threshold as a function of $pd$. In this simulation, only $p$ is changed while $d$ is fixed. The following are observed. In comparison with the DC Paschen law, a high $pd$ region has a smaller breakdown potential. The neglect of the

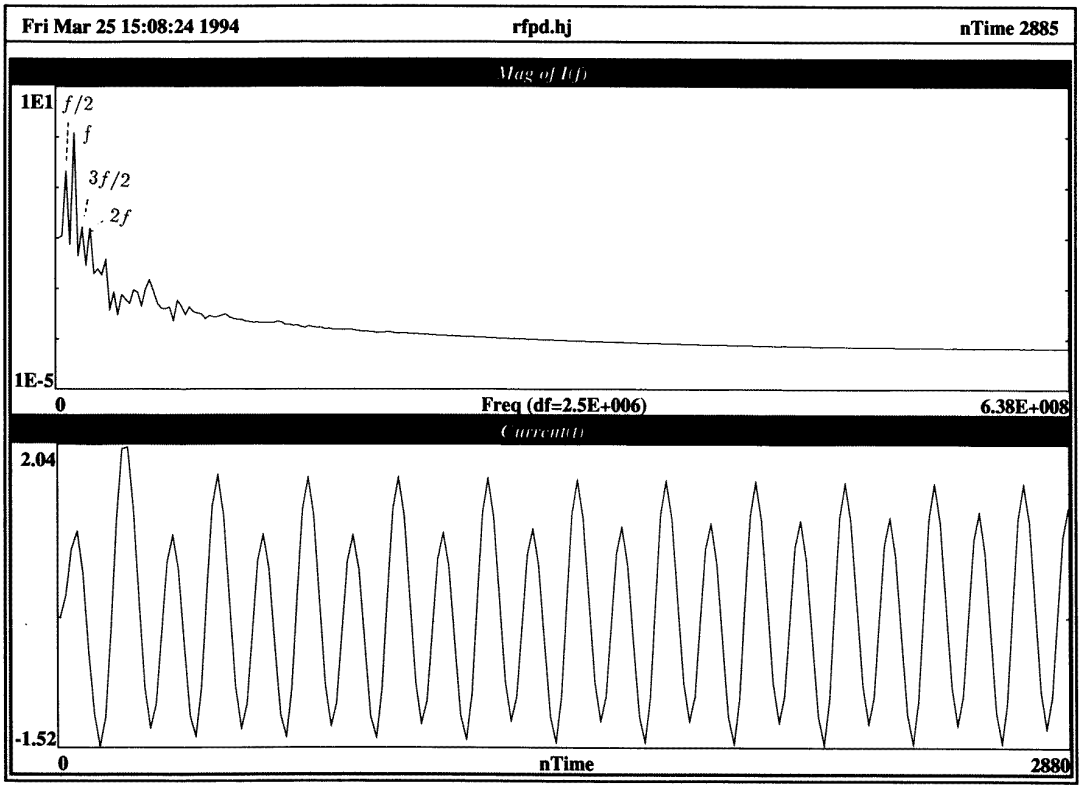


**Figure 2.** The discharge current waveform and its Fourier spectrum. The higher harmonics and sub-harmonics are shown and period doubling is also observed.

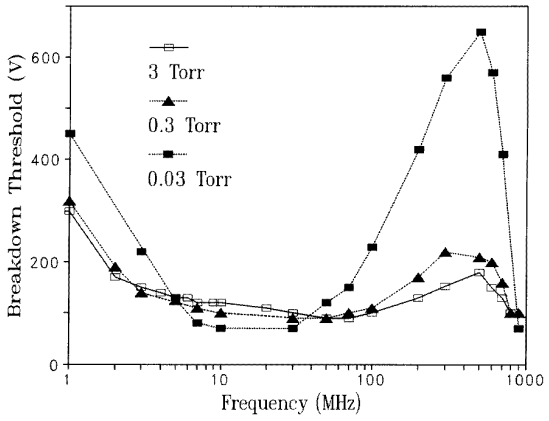


**Figure 3.** The breakdown voltage as a function of driver frequency for three different values of gas pressure, $p$ = 0.03, 0.3 and 3 Torr.

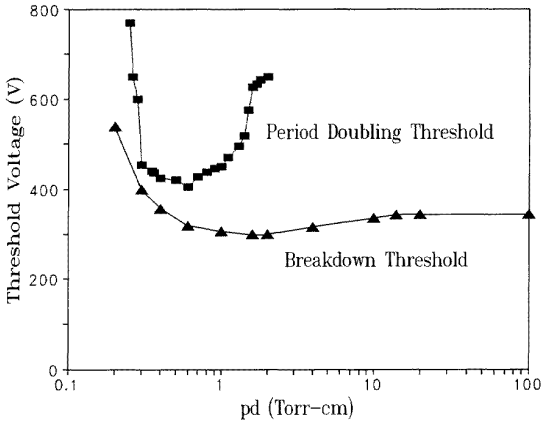


**Figure 4.** The breakdown voltage and the PD threshold as functions of *pd*.

recombination which becomes important for a high-pressure region is a possible cause for this discrepancy. It should be noted that the PD threshold is always higher than the breakdown threshold. Because the onset of PD causes the plasma sheath with nonlinear capacitance which is produced after the breakdown in gases, the results indicate that PD can take place after the breakdown. In comparison with previous results, the PD threshold has larger values than the results of Miller *et al* [8] for a high *pd* region. An analytical prediction solving equation (3) based on [8] also confirms this result. As observed before [8], the code does not converge to a stable steady state continuous PD mode and PD disappears after 10–20 RF cycles. Although this simulation assumes the constant gas temperature and uniform gas density, the RF heating effect increases the neutral gas temperature and destroy the uniformity of the gas density. This phenomenon precludes a meaningful comparison with experiment. The PD domain in the *pd*–period-doubling threshold voltage curvee has several windows in which PD is not found, but these windows are not shown in the present paper. This phenomenon is

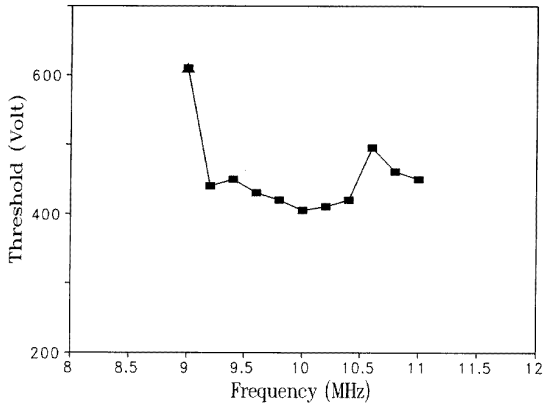


**Figure 5.** The PD threshold voltage as a function of the driver frequency.

another interesting topic to be investigated.

In figure 5, the PD threshold is shown with varying driver frequency over a large range around the resonance frequency which produces the lowest threshold. The results obtained are presented in a kind of phase diagram in two-dimensional parameter space $(f, V_{rf})$. Further increase in the excitation level beyond the PD threshold can lead to successive stages of period multiplication from which we may expect the onset of chaos at a finite excitation level.

Figure 6 shows changes in electrical signals that occur as the driving voltage, the control variable, is changed. Electrical signal data clearly show the 300–400 V transion region between different plasma modes. The current value $I(f)$ and voltage value $V(f)$ are the magnitudes of the Fourier-analysed components of the discharge current and potential at the mid-plane between the two electrodes at the indicated multiples of the driver frequency $f$. Over the 400–700 V range, the components of current at the driver frequency increases monotonically from 1.036 to 1.874 A; the second harmonic $2f$ is present, as expected, whether or not period doubling occurs. The onset of odd half harmonics signifies period-doubling bifurcations. It would be necessary to extend the RF voltages to higher values in search of further bifurcation and chaos. To drive the discharge system, an ideal voltage source producing a sinusoidal signal of fundamental frequency is chosen. However, once the plasma has been struck, there is a substantial harmonic content in the voltage of the powered electrode. This may lead to a chaotic regime.

The threshold level shown in figure 7 has a minimum at which the circuit is resonant at the sub-harmonic frequency. In this simple $RLC$ circuit model, an impedence pole near $f/2$ is the key feature that leads to a low threshold for period doubling. This arrangement produced the desired impedance pole near $f/2$. The total capacitance consisted of the external capacitance $C_{ext}$ in parallel with the plasma capacitance $C_0$. In order to adjust the resonance frequency of the circuit, a variable external capacitor is connected across the simple $RLC$ circuit. The code includes a series $RLC$ circuit that can be tuned to produce sub-harmonics. These variations successfully lead to observing PD with the PDS1 code. Figure 7 shows the PD threshold voltage

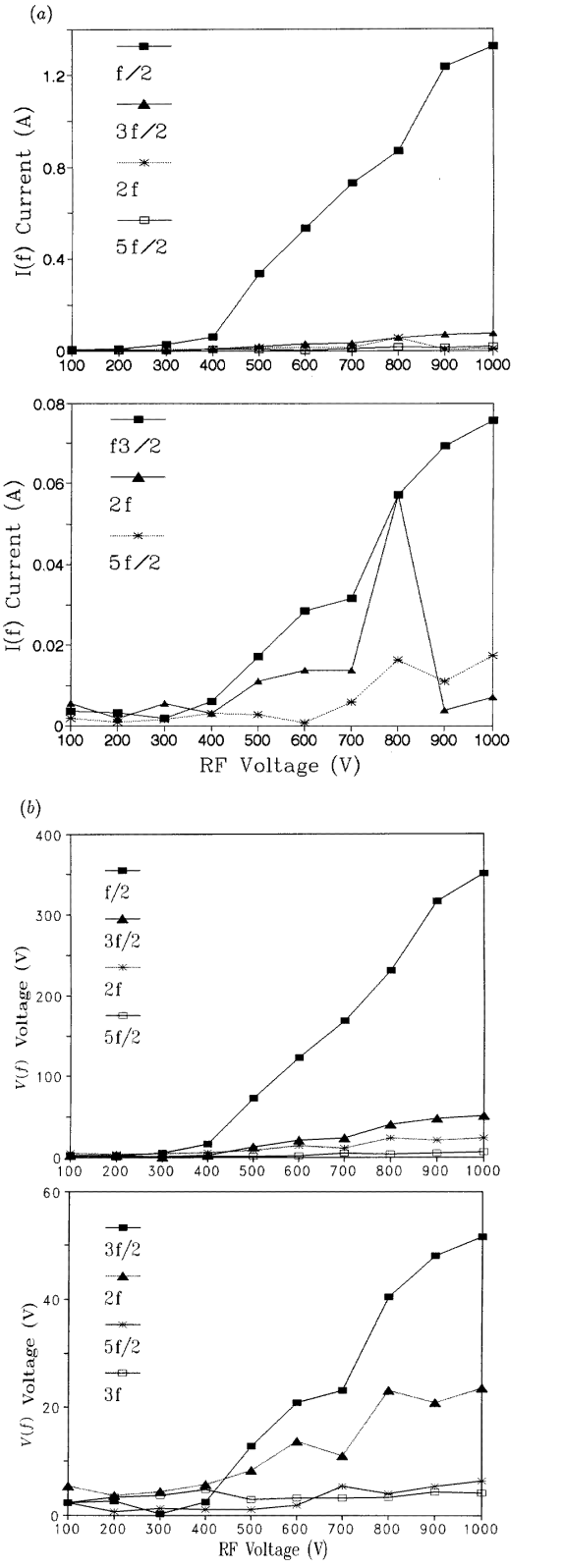


**Figure 6.** (*a*) The current magnitudes of the Fourier-analysed components $I(f)$ at the indicated multiples of the driver frequency as functions of the applied RF voltages. The onset of odd half harmonics signifies period-doubling bifurcations. (*b*) The voltage magnitudes of the Fourier-analysed components $V(f)$ as functions of the applied RF voltages.

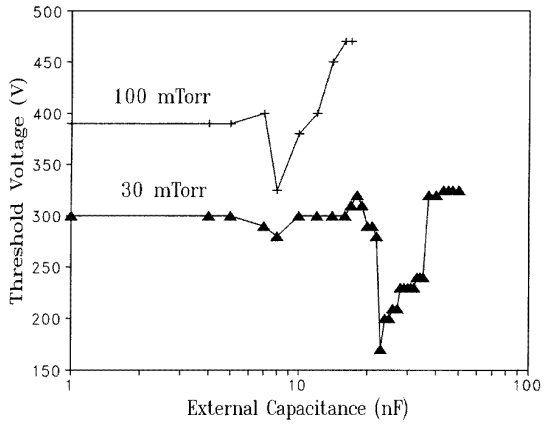


**Figure 7.** The calculated excitation threshold for sub-harmonic generation versus the tuning of the external capacitance. The impedance pole near $f/2$ is the key feature that leads to a low threshold for PD. The threshold is lowest when the circuit is resonant at the sub-harmonic frequency $f/2$.

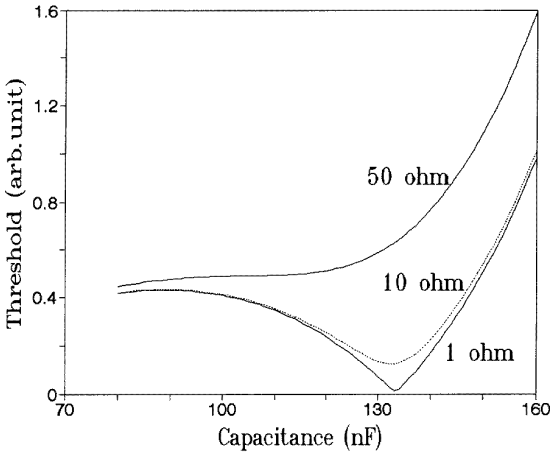


**Figure 8.** The analytically calculated PD threshold as a function of the capacitance for three cases of resistance.

determined at 30 and 100 mTorr. The data represent excitation levels just above the onset of sub-harmonics. The data are plotted as a function of circuit tuning as the external capacitance is varied. From figure 7 it can be noted that bifurcations are sensitive to parameters of the electrical circuit as well as to plasma-chamber conditions such as pressure, species and geometry.

The results of the analytical calculation employing equation (4) are shown in figure 8. Three values of the resistance of the circuit are used. As the resistance increases, the threshold pole (which is also shown in figure 7) disappears. Calculations of the variation of the PD threshold with varying pressure are presented in figure 9. Figure 9 shows the calculated external capacitance which produces the lowest threshold to the specific pressure value together with corresponding threshold voltage values. It should be noted that the resonant frequency of the circuit is determined from the total capacitance (consisting of external capacitance and plasma sheath capacitance), thus

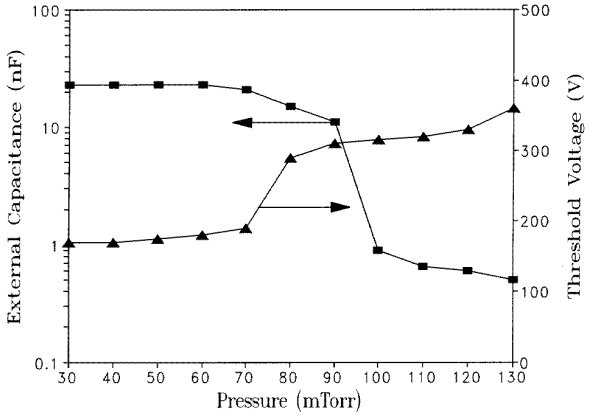


**Figure 9.** The pressure-dependence of the optimal external capacitance which produces the lowest PD threshold. The corresponding PD threshold values are shown together.

this plot can provide a proper estimation of the plasma sheath capacitance. This, in turn, gives the sheath thickness because the sheath capacitance is inversely proportional to the sheath thickness [10]. This plasma sheath capacitance is actually comprised of two sheaths (inner capacitance and outer capacitance) in series. In this study, the plasma sheath capacitance due to the sheath at the powered electrode is dominant.

Figure 10 shows the calculated sheath thickness as a function of pressure [11]. The result indicates that the plasma capacitance $C_0$ is increased as the pressure increases. In this simulation, the sheath thickness decreases with increasing plasma capacitance. These data apply to plasma at the edge of the period-doubling regime (plasma in which period doubling is not actually occurring). At intermediate gas pressures around 30–130 mTorr, the sheath thickness $d$ depends on the pressure $p$ according to the approximate expression $p^{1/6}d =$ constant. The simulation results performed for the parallel plate RF discharge show that, in the low-pressure region, (60–200 mTorr), $p^{0.32}d =$ constant, whereas, in the medium pressure region (200–500 mTorr) and above, $p^{0.5}d =$ constant [17]. The analytical derivation of $p^{1/6}d =$ constant is based on the collisional sheaths which are described by the collisional Child–Langmuir law [12] in the spherical geometry. However, we will discuss this problem in a subsequent paper.

## 4. Conclusions

The characteristics of a 10 MHz RF glow-discharge Ar plasma are studied by particle-in-cell simulation. A spherical plasma device using a one-dimensional plasma model is considered. The code determines the breakdown voltage, $V_{rf}$, for a given $pd$ and then compares these values with those from Paschen's law for the DC case. Also, the code calculates the breakdown voltage as a function of the driver frequency. In comparison with Paschen's law for the DC case, a high $pd$ part has smaller ignition potential, since the recombination is neglected in the simulation although this becomes important for a high-pressure region. The

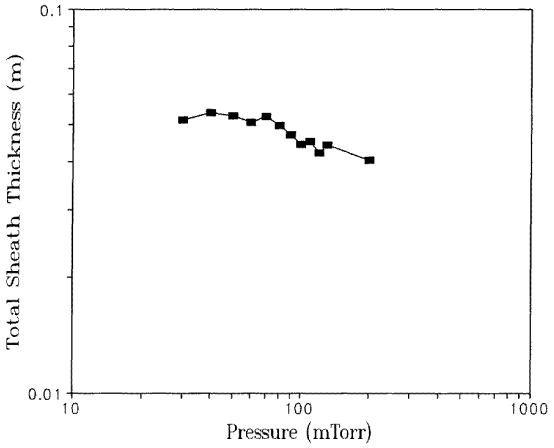


**Figure 10.** The sheath thickness as a function of gas pressure.

frequency-dependence of the breakdown voltage does not conflict with the prediction of the single-particle theory.

Plasma-sheath capacitance nonlinearity is the cause of PD in the RF discharge system. It is to be noted that the PD threshold is higher than the breakdown threshold. Because the onset of PD causes a plasma sheath with nonlinear capacitance which is produced after the breakdown in gases, the results indicate that PD can take place after the breakdown. The PD domain on the *pd*–period-doubling threshold curve has several windows in which PD is not found, but these are not presented in this paper. It is observed that a further increase in the RF voltage level beyond the PD threshold can lead to successive stages of period multiplication that result in the onset of chaos at a finite excitation level. The identification of possible routes to chaos is also an interesting topic. It is also noted that PD threshold measurements provide a novel diagnostics to determine plasma sheath capacitance. The modelling of the functional form of the equivalent capacitance by equation (4) provide a fairly good result which is also in agreement with the PIC simulation. Further study on the accurate model of the dependence of sheath capacitance on the applied RF voltage and driver frequency should be pursued.

## Acknowledgments

This work was supported in part by the South Korean Ministry of Education (Basic Science Research Institute Programme), the South Korean Science and Engineering Foundation and the Electronics and Telecommunication Research Institute.

## References

[1] Misium G R, Lichtenberg A J and Lieberman M A 1989 *J. Vac. Sci. Technol.* A **7** 1007
[2] Birdsall C K 1991 *IEEE Trans. Plasma Sci.* **19** 65
[3] Rhee M J and Ding B N 1992 *Phys. Fluids* B **4** 764
[4] Essam Nasser 1971 *Fundamentals of Gaseous Ionization and Plasma Electronics* (New York: Wiley)
Brown S C 1959 *Basic Data of Plasma Physics* (New York: AIP)
[5] Klinker T, MeyerIlse W and Lauterborn W 1984 *Phys. Lett.* **101A** 371
[6] Qin J, Wang L, Yuan D P, Gao P and Zhang B Z 1989 *Phys. Rev. Lett.* **63** 163
[7] Miller P A and Greenberg K E 1992 *Appl. Phys. Lett.* **60** 2859
[8] Miller P A, Romero L A and Pochan P D 1993 *Phys. Rev. Lett.* **71** 863
[9] Godyak V A 1986 *Soviet Radio Frequency Discharge Research* (Fall Church, VA: Delphic Associates)
Godyak V A, Piejak R B and Alexandrovich B M 1991 *IEEE Trans. Plasma Sci.* **19** 660
[10] Lieberman M A 1989 *IEEE Trans. Plasma Sci.* **17** 338
[11] Arbel D, Bar-Lev Z, Felsteiner J, Rosenberg A and Slutsker Ya Z 1993 *Phys. Rev. Lett.* **71** 2919
[12] Mutsukura N, Kobayashi K and Machi Y 1990 *J. Appl. Phys.* **68** 2657
[13] Verboncoeur J P, Vahedi V, Alves M V and Birdsall C K Plasma Theory and Simulation Group, Electronics Research Laboratory, Cory Hall, University of California, Berkeley, CA 94720
[14] Meyer P, Wunner G, Schmitt W and Ruder H P 1995 *Appl. Phys.* **77** 992
[15] Godyak V A, Piejak R B and Alexandrovich B M 1992 *Phys. Rev. Lett.* **68** 40
[16] Ferreira C M and Moisan M 1992 *Microwave Excited Plasmas* ed M Moisan and J Pelletier (Amsterdam: Elsevier) p 53
[17] Chung T H, Yoon H S and Lee J K 1995 *J. Appl. Phys.* **78** 6441